

Simultaneous measurement of nitric oxide production by conducting and alveolar airways of humans

ANTHONY P. PIETROPAOLI,¹ IRENE B. PERILLO,¹ ALFONSO TORRES,¹
 PETER T. PERKINS,¹ LAUREN M. FRASIER,¹ MARK J. UTELL,^{1,2}
 MARK W. FRAMPTON,^{1,2} AND RICHARD W. HYDE^{1,2}

Departments of ¹Medicine and ²Environmental Medicine, University of Rochester School of Medicine and Dentistry, Rochester, New York 14642-8692

Pietropaoli, Anthony P., Irene B. Perillo, Alfonso Torres, Peter T. Perkins, Lauren M. Frasier, Mark J. Utell, Mark W. Frampton, and Richard W. Hyde. Simultaneous measurement of nitric oxide production by conducting and alveolar airways of humans. *J. Appl. Physiol.* 87(4): 1532–1542, 1999.—Human airways produce nitric oxide (NO), and exhaled NO increases as expiratory flow rates fall. We show that mixing during exhalation between the NO produced by the lower, alveolar airways (\dot{V}_{LNO}) and the upper conducting airways (\dot{V}_{UNO}) explains this phenomenon and permits measurement of \dot{V}_{LNO} , \dot{V}_{UNO} , and the NO diffusing capacity of the conducting airways (D_{UNO}). After breath holding for 10–15 s the partial pressure of alveolar NO (PA) becomes constant, and during a subsequent exhalation at a constant expiratory flow rate the alveoli will deliver a stable amount of NO to the conducting airways. The conducting airways secrete NO into the lumen (\dot{V}_{UNO}), which mixes with PA during exhalation, resulting in the observed expiratory concentration of NO (PE). At fast exhalations, PA makes a large contribution to PE, and, at slow exhalations, NO from the conducting airways predominates. Simple equations describing this mixing, combined with measurements of PE at several different expiratory flow rates, permit calculation of PA, \dot{V}_{UNO} , and D_{UNO} . \dot{V}_{LNO} is the product of PA and the alveolar airway diffusion capacity for NO. In seven normal subjects, $PA = 1.6 \pm 0.7 \times 10^{-6}$ (SD) Torr, $\dot{V}_{LNO} = 0.19 \pm 0.07$ $\mu\text{l}/\text{min}$, $\dot{V}_{UNO} = 0.08 \pm 0.05$ $\mu\text{l}/\text{min}$, and $D_{UNO} = 0.4 \pm 0.4$ $\text{ml} \cdot \text{min}^{-1} \cdot \text{Torr}^{-1}$. These quantitative measurements of \dot{V}_{LNO} and \dot{V}_{UNO} are suitable for exploring alterations in NO production at these sites by diseases and physiological stresses.

nitric oxide diffusing capacity of airways; nitric oxide production by airways; lung nitric oxide; breath holding

INCREASED EXHALED nitric oxide (NO) concentrations have attracted interest as a means for detecting inflammation of the airways in asthma (17). NO production by the lungs may be abnormal in diseases such as sepsis, cirrhosis, primary pulmonary hypertension, and interstitial lung diseases (18, 21, 26, 27). The exhaled concentration of NO (PE) increases as expiratory flow

rates (\dot{Q}_E) fall (24), so \dot{Q}_E must be kept constant to obtain reproducible measurements of PE (Fig. 1). The reason for this flow dependence has recently been elucidated by Tsoukias and co-workers (28, 29). They show that during exhalation the mixing between NO from the lower alveolar airways perfused by the pulmonary circulation (\dot{V}_{LNO}) with NO produced in the upper conducting airways (\dot{V}_{UNO}) perfused by the bronchial circulation explains this phenomenon. Simple equations can describe this mixing. When combined with multiple measurements of PE at different \dot{Q}_E , these equations permit calculation of \dot{V}_{UNO} and the partial pressure of NO in the lower alveolar airways (PA). In this report, we describe an analysis of expired NO at different \dot{Q}_E that also permits calculation of the diffusing capacity of the upper airways (D_{UNO}) and \dot{V}_{LNO} . \dot{V}_{LNO} is determined from the product of PA and measurements of the pulmonary diffusing capacity of the lower airways (D_{LNO}) (12). Because diseases and physiological stress may cause changes in NO production and diffusing capacity by the alveoli different from those by the conducting airways, measurement of \dot{V}_{LNO} , \dot{V}_{UNO} , D_{LNO} , and D_{UNO} may provide new information about factors that alter NO production by the lungs.

Glossary

| | |
|-------------|--|
| D_{LNO} | Diffusing capacity of the lower, alveolar airways recorded as milliliters of NO STPD moving from the air spaces into the tissues and blood per minute per Torr of NO in the air spaces |
| D_{UNO} | Diffusing capacity of the upper, conducting airways recorded as milliliters of NO STPD moving from the air spaces into the tissues and blood per minute per Torr of NO in the air spaces |
| f | Small fraction of D_{UNO} , PU, or \dot{V}_{UNO} |
| FVC | Forced vital capacity |
| NO | Nitric oxide |
| PA | Partial pressure of NO in the alveoli |
| PB | Barometric pressure |
| PE | Partial pressure of NO in exhaled gas |
| PU | Partial pressure on NO in all or a segment of the upper conducting airway |
| \dot{Q}_E | Expiratory flow rate |

The costs of publication of this article were defrayed in part by the payment of page charges. The article must therefore be hereby marked "advertisement" in accordance with 18 U.S.C. Section 1734 solely to indicate this fact.

| | |
|-----------------|--|
| RV | Residual volume of gases in the lungs |
| TLC | Total capacity of gases in the lungs |
| \dot{V}_{LNO} | Rate of production of NO by the lower alveolar airways that enters the airways |
| \dot{V}_{UNO} | Rate of production of NO by the conducting airways that enters the airways |

METHODS

NO Exchange in the Alveolar Airways

The alveolar airways are defined as those tissues and air spaces well perfused by the pulmonary circulation, such as the alveoli, alveolar ducts, and respiratory bronchioles. In this zone, some of the NO produced by these lower airways diffuses into the air spaces. The fraction of the total NO produced in this alveolar compartment that enters the air spaces is called \dot{V}_{LNO} . The NO in the alveoli can react with the surrounding tissues (16) or diffuse rapidly through the alveolar capillary membrane into the perfusing blood. After elimination of ventilation by breath holding for 10–15 s, a steady state will develop, and the amount of NO entering the alveoli (\dot{V}_{LNO}) equals the amount of NO diffusing into the perfusing blood and surrounding tissues (12) or

$$\dot{V}_{LNO} = PA \cdot DL_{NO} \tag{1}$$

where DL_{NO} is the alveolar airway NO diffusing capacity, which is considered equivalent to the NO pulmonary diffusing capacity. Therefore, determination of PA multiplied by an independent measurement of DL_{NO} permits calculation of \dot{V}_{LNO} . DL_{NO} was determined by a modification of the constant single exhalation method for measuring the pulmonary carbon monoxide diffusing capacity (DL_{CO}) described by Newth and co-workers (19) and Perillo and co-workers (20). Multiple values of DL_{NO} are calculated during the exhalation and averaged.

NO Exchange in the Conducting Airways

The conducting airways are defined as those airways extending from the alveolar airways to the mouth. Strategies such as continuous positive pressure in the mouth (13, 24) or constant suction of gases from one nostril (9, 28, 29) can be used to avoid contamination of expired NO from the conducting airways by the much higher concentration in the nasophar-

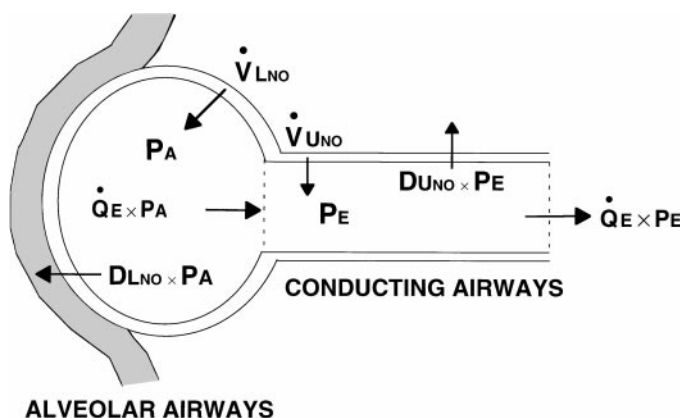


Fig. 2. Two-compartment model consisting of lower alveolar airways and upper conducting airways that assumes a constant concentration of NO within each compartment (*model 1*). After breath holding for 10–20 s, concentration of NO in alveolar airways (PA) becomes constant, because alveolar airway NO production (\dot{V}_{LNO}) then equals amount of NO diffusing out of airways, or $\dot{V}_{LNO} = DL_{NO} \cdot PA$, where DL_{NO} is diffusing capacity of NO in alveolar airways. During subsequent exhalation at a constant \dot{Q}_E , alveolar airways deliver a constant amount of NO to the conducting airways, which equals $PA \div (PB - 47)$, where PB is barometric pressure. \dot{V}_{LNO} mixes with NO production by conducting airways (\dot{V}_{UNO}), resulting in an NO concentration of PE . Some of PE diffuses back into tissues of conducting airways ($DU_{NO} \cdot PE$, where DU_{NO} is diffusing capacity for NO of conducting airways).

ynx (14). NO gas exchange in the conducting airways can be analyzed in the same manner as in the alveolar airways. Namely, a fraction of NO production by the conducting airways (\dot{V}_{UNO}) enters the lumen. Some of this NO can diffuse back into the tissues of the conducting airways and enter the bronchial circulation in proportion to the partial pressure of NO in the lumen of the conducting airways (PU). If the bronchial blood flow maintains the partial pressure of NO in the blood perfusing the tissues of the conducting airways at a negligible level, the amount of NO in the lumen that diffuses back into these tissues will equal $PU \cdot DU_{NO}$. With exhalation at a constant flow rate, PU will reach a constant value, and during this steady state \dot{V}_{UNO} will equal the amount of NO diffusing back into the tissues or

$$\dot{V}_{UNO} = PU \cdot DU_{NO} \tag{2}$$

We describe two models of the conducting airways based on the above assumptions that allow the simultaneous calculation of PA , \dot{V}_{UNO} , and DU_{NO} from multiple measurements of PE performed at different constant \dot{Q}_E .

Model 1. *Model 1* assumes a uniform concentration of NO throughout the conducting airways (Fig. 2), so $PU = PE$. After breath holding for 10–15 s, a constant PA is achieved (12), and subsequent exhalation at a steady flow rate (\dot{Q}_E) delivers a constant amount of NO to the conducting airways equal to $\dot{Q}_E [PA \div (PB - 47)]$, where PB is the barometric pressure, 47 is the partial pressure of water at body temperature in Torr, \dot{Q}_E is expressed in milliliters per minute STPD, and PA is expressed in Torr. This NO from the alveolar airways instantaneously mixes with NO in the conducting airways, resulting in a uniform partial pressure of NO in the conducting airways and the expired breath (PE). The amount of NO exhaled at any instant (STPD) equals $\dot{Q}_E [PE \div (PB - 47)]$. This equals the contribution from the alveolar airways [$\dot{Q}_E [PA \div (PB - 47)]$] plus \dot{V}_{UNO} less the NO diffusing from the lumen of the conducting airways back into the tissues and bronchial

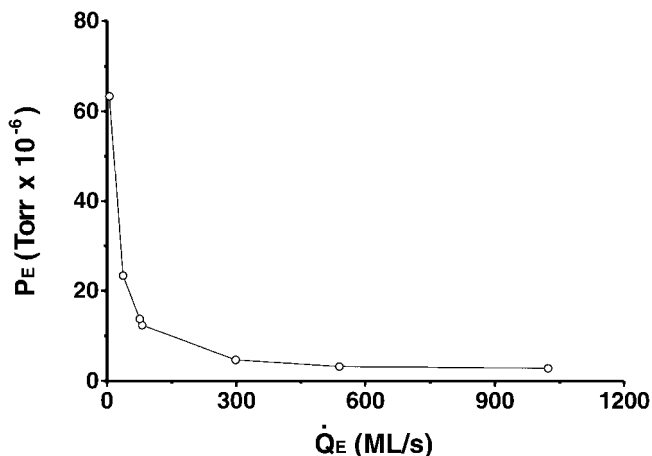


Fig. 1. Exhaled nitric oxide (NO) (PE) vs. flow rate (\dot{Q}_E) in normal subject AP after 15 s of breath holding. Note marked decrease in PE as flow rates increase.

circulation of the conducting airways ($PE \cdot DU_{NO}$) or

$$\dot{Q}_E \cdot \frac{PE}{PB - 47} = \dot{Q}_E \cdot \frac{PA}{PB - 47} + \dot{V}_{UNO} - (PE \cdot DU_{NO}) \quad (3)$$

Rearranging gives

$$PE = \frac{1}{\dot{Q}_E} [\dot{V}_{UNO} - PE \cdot DU_{NO}] (PB - 47) + PA \quad (4)$$

Multiple sets of measurements of PE at different \dot{Q}_E provide the data needed to determine PA , \dot{V}_{UNO} , and DU_{NO} in *Eqs. 3* and *4*. First, PA is determined graphically by taking advantage of the following observation: At higher values of \dot{Q}_E (i.e., >200 ml/s), PE is relatively small and results in the term $PE \cdot DU_{NO}$ decreasing to $<3\%$ of \dot{V}_{UNO} . If $PE \cdot DU_{NO}$ is considered insignificant at such flow rates, *Eq. 4* becomes

$$PE = \frac{1}{\dot{Q}_E} [\dot{V}_{UNO} (PB - 47)] + PA \quad (5)$$

Equation 5 has the following form: $y = mx + b$. A plot of PE vs. $1/\dot{Q}_E$ results in PA at the y -intercept when $1/\dot{Q}_E = 0$, which is also the point where $\dot{Q}_E = \infty$. The slope equals $\dot{V}_{UNO}(PB - 47)$. We therefore calculated PA from the linear regression of PE plotted vs. $1/\dot{Q}_E$ when $\dot{Q}_E > 200$ ml/s (Fig. 3). If these data failed to result in a doubling of PE , data at the next slower flow rate <200 ml/s were added until PE doubled its lowest value. This value of PA was combined with all the measurements of PE and \dot{Q}_E collected at different constant \dot{Q}_E to calculate the remaining two variables, \dot{V}_{UNO} and DU_{NO} , with use of *Eq. 4* with the assistance of a curve-fitting program utilizing a quasi-Newton regression (8) (Fig. 4). The program forced the fit through the calculated value of PA . To determine whether the quasi-Newton regression-fitting algorithm supplied a unique solution for \dot{V}_{UNO} and DU_{NO} , we also calculated their values using the Newton and the steepest descent-fitting algorithms for a representative subject. The three algorithms yielded the same values for \dot{V}_{UNO} and DU_{NO} . Therefore, the choice of curve-fitting algorithm does not influence identification of the unique solutions from these data. The curve-fitting program requires assumed starting values for \dot{V}_{UNO} and DU_{NO} . These were arbitrarily chosen to be $0.1 \mu\text{l}/\text{min}$ and $0.3 \text{ ml} \cdot \text{min}^{-1} \cdot \text{Torr}^{-1}$, respectively. In a representative subject, these starting values could be systematically varied 4- to 10-fold before deterioration of the fitted

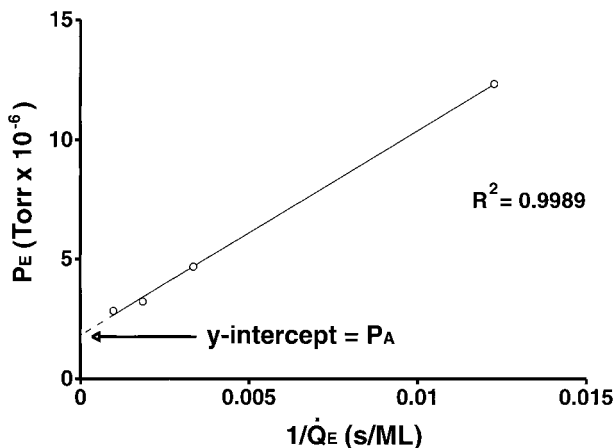


Fig. 3. PE vs. reciprocal of \dot{Q}_E ($1/\dot{Q}_E$) for 4 fastest exhalations by *subject AP*. Note linear relationship between different pairs of values of PE and $1/\dot{Q}_E$. Extrapolation of line of least mean squares to $1/\dot{Q}_E = 0$ (i.e., $\dot{Q}_E = \infty$) results in $PA = 1.8 \times 10^{-6}$ Torr.

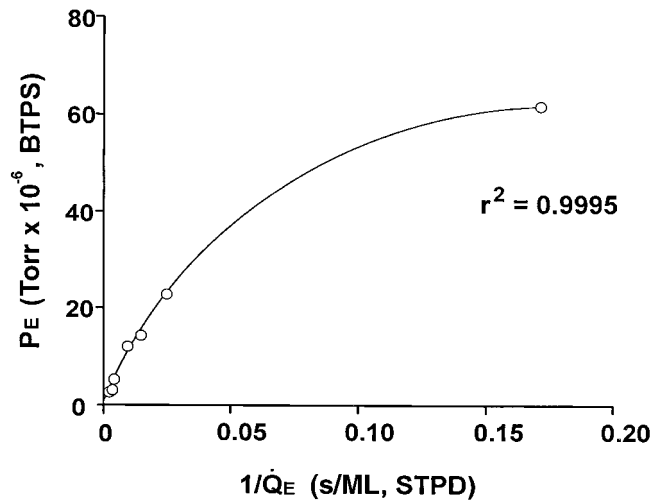


Fig. 4. PE vs. $1/\dot{Q}_E$ with use of same data from *subject AP* in Fig. 1. y -Intercept, where $1/\dot{Q}_E = 0$ (i.e., $\dot{Q}_E = \infty$) equals PA and was determined from a linear extrapolation with a linear regression through 4 fastest values for \dot{Q}_E in Fig. 3. Computer then used this value for PE and all 7 data points with *Eq. 4 (model 1)* or *Eq. 7 (model 2)* to determine \dot{V}_{UNO} and DU_{NO} . Solid curved line is computer solution that uses *Eq. 5*. Both models resulted in similar close fits to data, with $r^2 > 0.998$ in all subjects. As slope of curve becomes steeper, \dot{V}_{UNO} increases. As curvature increases, DU_{NO} increases.

curve became apparent. If a poor fit is obtained, starting values would need to be changed to allow the program to identify a reasonable fit to the data.

To determine whether a reliable measurement of \dot{V}_{UNO} was possible from just the faster values of \dot{Q}_E used to calculate PA , \dot{V}_{UNO} was also calculated from these data with *Eq. 5* and compared with \dot{V}_{UNO} determined with all values of \dot{Q}_E by use of *Eq. 4*.

This method for measuring PA , \dot{V}_{UNO} , and DU_{NO} with *model 1* assumes rapid arrival at a new steady state when the NO coming from the alveolar airways mixes with the NO in the conducting airways during exhalation. APPENDIX A describes an equation for calculating the changes in PE during mixing and shows the amount of gas needed to be exhaled to reach a steady state. The equation shows that once $\sim 30\%$ of the expiratory vital capacity has been exhaled after the initial breath-holding period, PE is within 99% of the constant equilibrated value, so *Eqs. 4* and *5* are valid for measuring PA , \dot{V}_{UNO} , and DU_{NO} .

Model 2. *Model 2* assumes stratification of the NO concentration in the conducting airways so the concentration of NO can gradually increase as the expired gas moves through the conducting airway (Fig. 5). In contrast to *model 1*, the conducting airway is considered to be a cylinder with a total volume K and an infinite number of uniform segments. Each segment has an equal fraction (f) of K , \dot{V}_{UNO} , and DU_{NO} , so that the dimensions of any segment are fV , $f\dot{V}_{UNO}$, and fDU_{NO} . At the start of exhalation at a constant \dot{Q}_E , PA enters the first segment, where $f\dot{V}_{UNO}$ adds NO and fDU_{NO} removes NO at a rate proportional to the partial pressure of NO in the segment. The bronchial blood flow in the wall of the upper airway is assumed to keep its partial pressure of NO at a negligible level. The resultant partial pressure of NO in the lumen of the segment equals PU_1 . PU_1 then enters the next segment, and its fraction of \dot{V}_{UNO} and DU_{NO} results in PU_2 , and so forth. At the proximal end of the conducting airway, $PU = PE$.

For any segment of the conducting airways, the amount of NO in the segment of volume fK equals $fK[PU \div (PB - 47)]$. It is changed by the NO production ($f\dot{V}_{UNO}$) entering the seg-

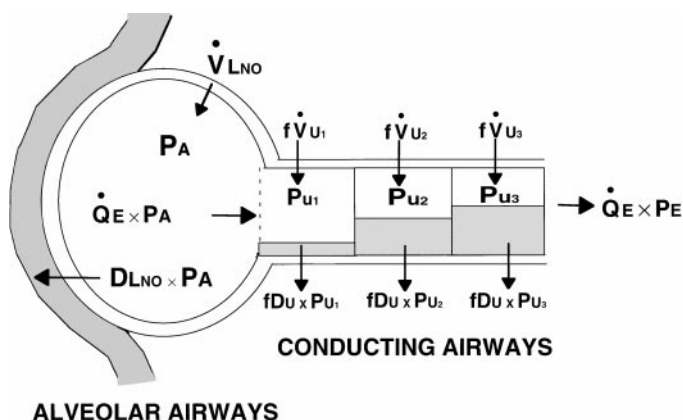


Fig. 5. Model of lower alveolar airways and upper conducting airways that assumes a progressive change in partial pressure of NO in conducting airways (PU) during exhalation (model 2). In contrast to model 1 in Fig. 2, conducting airways are divided into an infinite number of segments, each with same fraction (f) of conducting airway volume, conducting airway NO production (fV̇_U), and conducting airway diffusing capacity (fDU). In 1st segment, fV̇_U adds NO to lumen and fDU_{NO} removes NO, resulting in a partial pressure of NO equal to P_{U1}. P_{U1} then moves to next segment, where fV̇_U and fDU result in P_{U2}. At end of conducting airway, final value for P_U equals P_E. Other symbols are identified in Fig. 2. See text and APPENDIX B for more details.

ment less the amount diffusing out (P_U · fDU_{NO}) or

$$\frac{d}{dt} fK \frac{P_U}{P_B - 47} = \dot{V}_{U_{NO}} - P_U \cdot fDU_{NO} \quad (6)$$

The solution of Eq. 6 given in detail in APPENDIX B is

$$P_E = \left(\frac{\dot{V}_{U_{NO}}}{DU_{NO}} - P_A \right) \left[1 - e^{-\frac{DU_{NO} (P_B - 47)}{\dot{Q}_E}} \right] + P_A \quad (7)$$

P_A is obtained from data obtained at the faster \dot{Q}_E , as described above. With this value of P_A and all the measured pairs of P_E and \dot{Q}_E , $\dot{V}_{U_{NO}}$ and DU_{NO} are calculated using Eq. 7 with the assistance of a curve-fitting program utilizing a quasi-Newton regression (8).

Measurement of NO

Details of methods for measuring NO have been recently published (9). Briefly, a rapidly responding chemiluminescence NO analyzer (Sievers NOA, model 270B, Sievers, Boulder, CO) operating at a sample rate of 250 ml/min measured exhaled levels of NO at the mouthpiece with a 150-cm-long, 1.6-mm-ID, 3.2-mm-OD Tygon inlet tube. Response time of the analyzer was <200 ms for a signal 90% of full scale. The analyzer was adjusted to provide 40 measure-

ments of the NO concentration per second that could be averaged over any time interval. The NO analyzer was calibrated daily by serial dilutions of a gas containing 229 parts per billion (ppb) of NO. To obtain gas samples free of NO, air from a gas cylinder containing <2 ppb of NO (Scott Specialty Gases, Plumsteadville, PA) was passed through a filter constructed from a 5.8-cm-ID, 19-cm-long cylinder (Gas Drying Unit, VWR Scientific, Rochester, NY) packed with potassium permanganate (Purafil, Thermoenvironmental Instruments, Franklin, MA) (4).

Because the air signal free of NO could drift as much as 2 ppb in 10 min, measurements of NO-free air were performed within 1 min before and after each NO measurement from expired gas samples, and these values were averaged to obtain the zero NO signal. The lag time between the volume signal obtained from a potentiometer attached to the spirometer and the change in the NO signal was determined daily and equaled 0.8 ± 0.1 (SD) s. Multiple repetitive measurements of gas mixtures of 2.8 and 8.2 × 10⁻⁶ Torr of NO showed a standard deviation of 0.09 × 10⁻⁶ Torr. We assumed that the detection limit of our analyzer was two times the standard deviation of these multiple measurements or 0.2 × 10⁻⁶ Torr. During gas sampling the operator exhaled warm humidified gas from the mouth by the inlet of the NO analyzer approximately every 5–10 min, so the walls of the unheated inlet tubing were kept moist. This resulted in all gases being considered measured at ATPS. Measurements of NO in parts per billion ATPS were converted to partial pressure of NO in Torr BTPS as follows: NO in Torr = (NO in ppb ATPS)(P_B)(P_B - 47) ÷ (P_B - P_{H₂O})(10⁹), where P_{H₂O} is partial pressure of water at room temperature. For example, at P_B of 760 Torr and room temperature of 24°C where P_{H₂O} = 22.4 Torr, 1 ppb NO = 0.735 × 10⁻⁶ Torr of NO. The chart recorder (MacLab Recording Instrument, AD Instruments, Castle Hill, Australia) stored the volume signal and NO signal in a Macintosh LC computer (Apple Computer, Cupertino, CA). To obtain a stable constant value for the measurement of P_E after breath holding, we discarded an initial portion of the exhalate equal to four times the sum of the subject's estimated anatomic dead space and the instrument dead space of 100 ml, as well as the final 10% of the exhalate (Fig. 6). At flow rates <45 ml/s, a constant value for P_E was obtained earlier during exhalation (APPENDIX A). At flow rates >1,000 ml/s, a constant value for P_E was frequently not present until 40–50% of the breath had been expired. In these cases, the NO plateau level was determined by visual assessment of the NO signal displayed on the computer.

Maneuvers Used to Measure P_E and \dot{Q}_E

Subjects exhaled to residual volume (RV) through the mouthpiece of the apparatus into the room and then rapidly

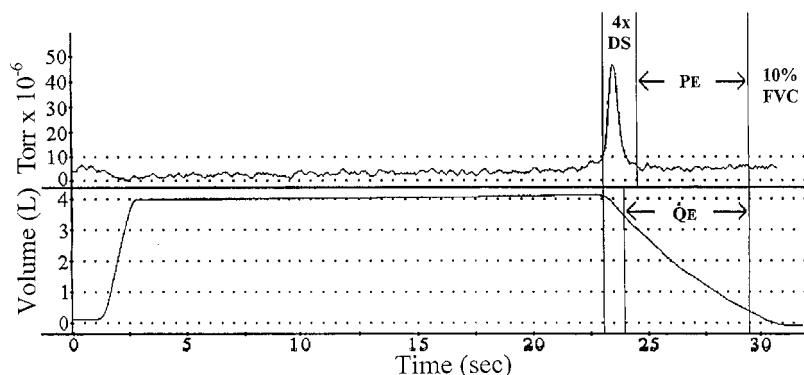


Fig. 6. Record of NO concentration at mouth (P_E) and lung gas volume signal during 20 s of breath holding followed by exhalation at 600 ml/s. P_E is obtained from NO plateau that follows NO peak seen at start of exhalation. Peak is attributed to accumulation of NO in conducting airways during breath holding that is then flushed through mouthpiece at beginning of exhalation. Data for calculating P_E was obtained after an initial expired volume equal to 4 times subject's and instrument's dead space (DS), as well as final 10% of forced vital capacity (FVC) was discarded. \dot{Q}_E was calculated from volume signal after initial and final 10% of FVC was discarded. NO signal was moved to left by 0.8 s to correct for lag between NO and volume signals.

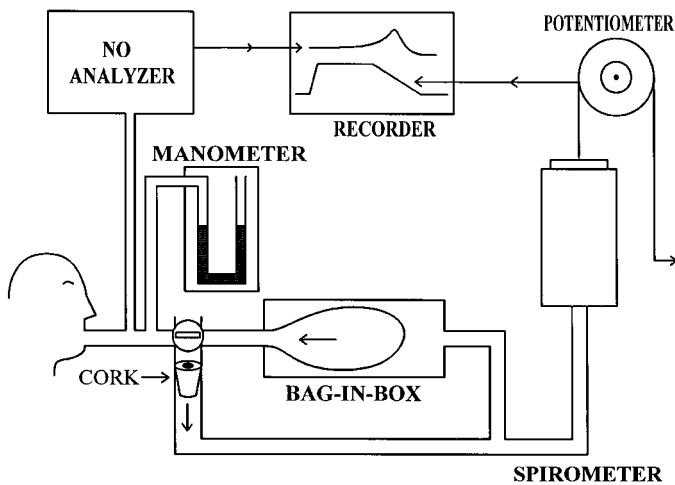


Fig. 7. Apparatus for measuring NO production of conducting and alveolar airways. After exhalation to residual volume, subject is connected via valve at mouthpiece to bag-in-box apparatus filled with room air and inspires to total lung capacity. After breath is held for 10–20 s, valve is turned 90° into spirometer circuit, and subject exhales, maintaining a mouth pressure of +5 cmH₂O by watching water manometer. Corks with different-sized apertures were placed in expiratory tubing and provided variable resistance to exhalation, resulting in different constant \dot{Q}_E . NO concentration is continuously measured via side port on mouthpiece. Changes in gas volume are measured with a spirometer attached to a potentiometer. NO and volume signals are displayed on a chart recorder and stored in a computer.

inhaled room air from a bag-in-box device to total lung capacity (TLC) (Fig. 7). The subject then held this breath for 10–20 s, so that P_A reached a constant concentration irrespective of the inhaled ambient NO concentration (12). At the end of the breath hold, the mouthpiece valve was turned 90° into the spirometry circuit, and the subject exhaled, maintaining mouth pressure at +5 cmH₂O by watching a water manometer. Corks with various-sized holes bored through their centers were placed in the expiratory tubing and resulted in different expiratory resistances and \dot{Q}_E . Each subject performed measurements at seven different flow rates that were as low as 6 ml/s and as high as 1,355 ml/s. Exhalations at each flow rate were performed in triplicate, and the values for P_E and \dot{Q}_E were averaged. P_E was measured as described above, and \dot{Q}_E was obtained from the spirometer's volume signal after the initial and final 10% of the expired volume were discarded (Fig. 6). The entire experiment for each subject was completed within 4 h on the same day.

Measurement of DL_{NO}

DL_{NO} for each subject was calculated from the expired NO concentration measured after inspiring 10 parts/million of NO in air placed in the bag in Fig. 7 from RV to TLC, breath holding for 5 s, and then exhaling to RV at a constant flow rate of 500 ml/s with a modification of the single-breath exhalation method for continuously measuring DL_{CO} during exhalation described by Newth and co-workers (19) and Perillo and co-workers (20). Lung volume at any instant during exhalation used in the calculation of the multiple values of DL_{NO} was obtained by adding the amount of exhaled gas remaining above RV recorded by the spirometer (Fig. 7) to the subject's RV. RV was obtained from the subject's functional residual capacity (FRC) measured with body plethysmography (5) by subtracting the expiratory reserve volume obtained from a spirometer (P. K. Morgan, Haverhill, MA) from FRC. The multiple measurements of DL_{NO} during the exhalation were

averaged and performed in triplicate, and the mean value was recorded.

Subjects

P_A , $\dot{V}_{U_{NO}}$, and $D_{U_{NO}}$ were measured in seven healthy, nonsmoking, 31- to 72-yr-old (mean 46 ± 18 yr) subjects. Five were men and two were women. All subjects were free of cardiopulmonary disease. Spirometry showed values >90% of predicted for the forced expiratory volume in 1 s, with a mean value of 104 ± 16 (SD)% (2). This study was approved by the University of Rochester's committee for investigations involving human subjects.

Statistical Methods

Values are means \pm SD. In experiments where subjects served as their own control, results were compared using a two-tailed paired *t*-test. Groups of subjects were compared with an unpaired *t*-test. $P < 0.05$ was required for statistical significance. Regression lines and curves were fitted to the experimental data by the line of least mean squares referenced to P_E .

RESULTS

P_A , $\dot{V}_{L_{NO}}$, and DL_{NO}

Figure 8 shows the values for P_E and the reciprocal of \dot{Q}_E ($1/\dot{Q}_E$) used to determine P_A from the faster exhalations in the seven subjects. The linear regression of these points extrapolated to infinite flow, where $1/\dot{Q}_E = 0$, equals P_A . The regression line fitted the data closely, with $r^2 = 0.965$ – 0.999 . P_A was $1.6 \pm 0.7 \times 10^{-6}$ (SD) Torr. DL_{NO} was 123 ± 19 ml·min⁻¹·Torr⁻¹. $\dot{V}_{L_{NO}}$ (i.e., $P_A \cdot DL_{NO}$) was 0.19 ± 0.07 μ l/min.

$\dot{V}_{U_{NO}}$ and $D_{U_{NO}}$

Figure 9 shows the paired values for P_E and $1/\dot{Q}_E$ for all exhalations by the seven subjects used to determine $\dot{V}_{U_{NO}}$ and $D_{U_{NO}}$. \dot{Q}_E ranged from 6 to 1,355 ml/s. For *model 1*, $\dot{V}_{U_{NO}}$ was 0.077 ± 0.053 μ l/min and $D_{U_{NO}}$ was 0.4 ± 0.4 ml·min⁻¹·Torr⁻¹; for *model 2* the values were similar: 0.074 ± 0.052 μ l/min and 0.5 ± 0.4 ml·min⁻¹·Torr⁻¹, respectively. The regression lines for both models fit the data closely, with $r^2 > 0.998$ in all subjects. The value of r^2 for the two models did not differ

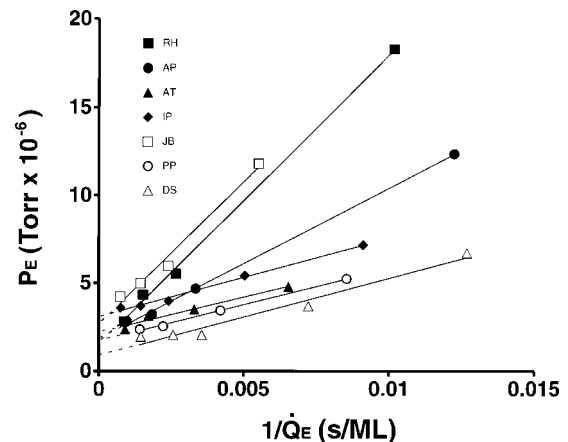


Fig. 8. P_E vs. reciprocal of faster values of \dot{Q}_E in 7 healthy subjects. Extrapolation of linear regression for each subject to infinite flow ($1/\dot{Q}_E = 0$) provided P_A on vertical axis. Slope equals $\dot{V}_{U_{NO}}(P_B - 47)$. See Eq. 5. Seven subjects represented by different symbols.

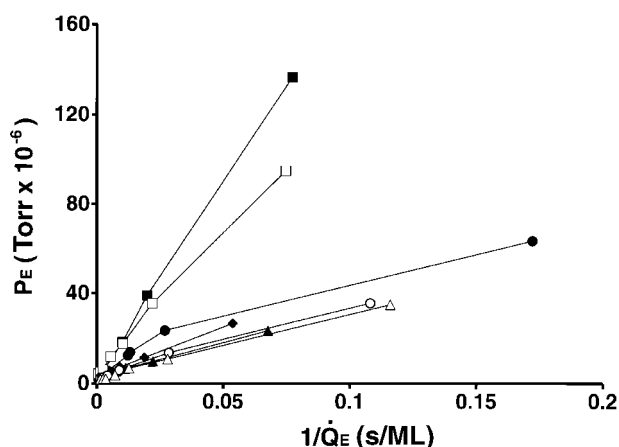


Fig. 9. PE vs. $1/\dot{Q}_E$ in 7 healthy subjects. Note linear relationship between PE and $1/\dot{Q}_E$ at faster \dot{Q}_E seen more clearly in Fig. 8. Straight lines connecting data points become less steep as $1/\dot{Q}_E$ increases (or \dot{Q}_E decreases), because higher values for PE at slower \dot{Q}_E result in more NO diffusing into walls of conducting airways. Different symbols identify each subject (see Fig. 8).

significantly: 0.9996 ± 0.0003 for *model 1* and 0.9994 ± 0.0006 for *model 2* ($P = 0.30$). $\dot{V}_{U_{NO}}$ calculated with just the faster values of \dot{Q}_E shown in Fig. 8 with use of Eq. 4 was 0.070 ± 0.048 $\mu\text{l}/\text{min}$. Although this value is slightly lower than 0.077 ± 0.053 $\mu\text{l}/\text{min}$ with *model 1* and 0.074 ± 0.052 $\mu\text{l}/\text{min}$ with *model 2*, the difference was not significant ($P = 0.2$).

Comparison of $\dot{V}_{L_{NO}}$ and $\dot{V}_{U_{NO}}$

Figure 10 shows that $\dot{V}_{L_{NO}}$ of 0.19 ± 0.07 $\mu\text{l}/\text{min}$ was consistently greater than $\dot{V}_{U_{NO}}$ of 0.077 ± 0.053 $\mu\text{l}/\text{min}$ with use of *model 1* ($P < 0.01$). Calculating with *model 2* gave similar results. $\dot{V}_{L_{NO}}$ was 0.19 ± 0.07 $\mu\text{l}/\text{min}$ compared with $\dot{V}_{U_{NO}}$ of 0.074 ± 0.052 $\mu\text{l}/\text{min}$ ($P < 0.01$).

Comparison of $D_{L_{NO}}$ and $D_{U_{NO}}$

Table 1 shows that $D_{L_{NO}}$ is >100 -fold greater than $D_{U_{NO}}$ calculated with *model 1* or *model 2*.

DISCUSSION

These data show that a model of the human airways where exhaled NO from the alveoli mixes with the NO

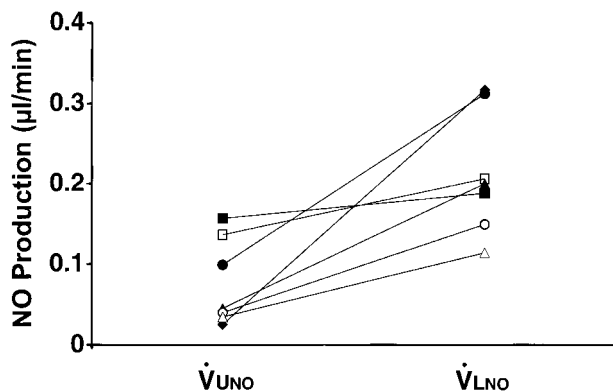


Fig. 10. $\dot{V}_{U_{NO}}$ (calculated using *model 1*) vs. $\dot{V}_{L_{NO}}$ in 7 healthy subjects. In all subjects, $\dot{V}_{L_{NO}}$ exceeded $\dot{V}_{U_{NO}}$, and difference was significant ($P < 0.01$). *Model 2* gave similar results ($P < 0.01$).

Table 1. $D_{L_{NO}}$ and $D_{U_{NO}}$ calculated with models 1 and 2 in healthy subjects

| | Mean \pm SD | Range |
|----------------|---------------|----------|
| $D_{L_{NO}}$ | 123 ± 19 | 92–147 |
| $D_{U_{NO}}$ | | |
| <i>Model 1</i> | 0.4 ± 0.4 | 0.04–1.1 |
| <i>Model 2</i> | 0.5 ± 0.4 | 0.08–1.2 |

Values are expressed in $\text{ml} \cdot \text{min}^{-1} \cdot \text{Torr}^{-1}$; $n = 7$. $D_{L_{NO}}$, diffusing capacity of alveolar airways; $D_{U_{NO}}$, diffusing capacity of conducting airways.

produced by the conducting airways precisely predicts the PE observed at different \dot{Q}_E . Simple equations describing this mixing combined with values for PE at different values of \dot{Q}_E result in measurements of $\dot{V}_{U_{NO}}$, $D_{U_{NO}}$, and PA. PA multiplied by a separate measurement of $D_{L_{NO}}$ gives a measurement of $\dot{V}_{L_{NO}}$. Besides these separate quantitative measurements of $\dot{V}_{L_{NO}}$ and $\dot{V}_{U_{NO}}$, this model provides a reasonable physiological explanation for the rise in expired NO with slower \dot{Q}_E and helps define the physiological basis for observed values of expired NO reported by many investigators (6, 13, 17, 24, 29).

Common practice is to measure expired NO at a single relatively slow \dot{Q}_E on the order of 100–250 ml/s (13). The resultant observed values of PE are three to five times PA and, therefore, predominantly represent $\dot{V}_{U_{NO}}$. Although these measurements at single relatively slow \dot{Q}_E values provide a useful index of $\dot{V}_{U_{NO}}$, they are at a disadvantage for detecting changes in PA and $\dot{V}_{L_{NO}}$.

A number of studies suggest that the mechanisms altering $\dot{V}_{U_{NO}}$ and $\dot{V}_{L_{NO}}$ may be different. The large increases in PE seen in bronchial asthma likely come from upregulation of inducible NO synthase in the conducting airways (11, 30). Endothelial-derived NO synthase is reported to be located in the alveolar capillary membrane (10) and is upregulated in a rat model of the hepatopulmonary syndrome (7). This upregulation could explain the high levels of exhaled NO observed in some patients with cirrhosis and the hepatopulmonary syndrome (18). Downregulation of endothelial-derived NO synthase may account for the low levels of expired NO reported in primary pulmonary hypertension (3, 21). The technique described in this report for measuring $\dot{V}_{U_{NO}}$ and $\dot{V}_{L_{NO}}$ should provide a quantitative method to localize alteration in NO production to the alveoli or the conducting airways. Such measurements may result in more precision in the use of exhaled NO to assess lung injury or alterations in regulation of NO production by the lungs than that obtained with observations at a single \dot{Q}_E .

Choice of Lung Models to Explain the Change in PE With Different Values of \dot{Q}_E

The simpler model (*model 1*) of the airways, where the conducting airways are considered one single uniform compartment, precisely described the observed data obtained at different values of \dot{Q}_E , with $r^2 > 0.998$ in all subjects. The multicompartiment model of the conducting airways (*model 2*), with the more realistic

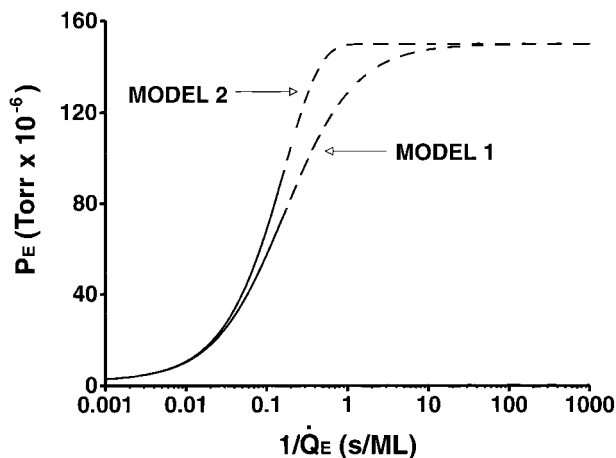


Fig. 11. Theoretical values for P_E at different constant \dot{Q}_E vs. $1/\dot{Q}_E$ for *models 1* and *2* (dashed curves). Assumed values were 2.0×10^{-6} Torr for P_A , $0.075 \mu\text{l}/\text{min}$ for $\dot{V}_{U\text{NO}}$, and $0.5 \text{ ml} \cdot \text{min}^{-1} \cdot \text{Torr}^{-1}$ for $D_{U\text{NO}}$. Solid curves represent realistically obtainable values for P_E in human subjects, where $\dot{Q}_E > 5 \text{ ml/s}$. Note similarity of shape of solid curves generated by *models 1* and *2*. This similarity makes it difficult to distinguish *models 1* and *2* by use of measurements of exhaled NO and \dot{Q}_E .

assumption that NO concentration in the conducting airways gradually approaches P_E during exhalation, does not provide a better fit to the observed data. We also performed theoretical calculations to see if measurements of P_E at \dot{Q}_E in humans as low as the practical limit of $\sim 5 \text{ ml/s}$ can be used to distinguish between the two models. These models generate different values for P_E shown in Fig. 11 for the same assumed values of P_A , $\dot{V}_{U\text{NO}}$, and $D_{U\text{NO}}$. Fitting the equation of one model to the data generated by the other model results in a very tight fit, with $r^2 > 0.999$ (Fig. 12). Therefore, observed values of P_E measured over a wide spectrum of \dot{Q}_E values cannot be expected to distinguish which model provides a more realistic prediction of the observed data.

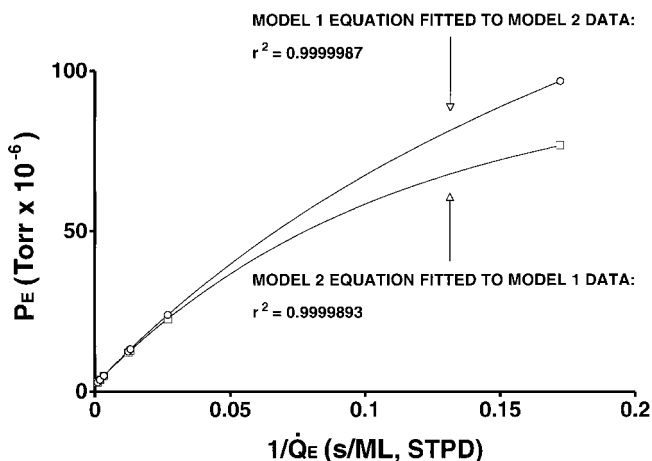


Fig. 12. Theoretical values of P_E vs. $1/\dot{Q}_E$ generated by *models 1* and *2* by use of assumed values for P_A , $\dot{V}_{U\text{NO}}$, and $D_{L\text{NO}}$ in Fig. 11 legend. $\dot{Q}_E = 1,000, 540, 300, 80, 75, 40,$ and 6 ml/s . Fitting *model 1* to data generated by *model 2* and vice versa results in very tight fits, with $r^2 > 0.999$. Because fits are so precise, observed data cannot be used to distinguish which model most closely predicts observed changes in P_E at different values of \dot{Q}_E .

Models 1 and *2* have limitations in their assumed dimensions, because the conducting airways must contain multiple compartments where the ratio of the surface area of the conducting airways that secretes NO into the gas volume in the lumen decreases as exhaled gas moves from the alveoli through the trachea (6, 23, 31). This anatomy results in uneven distribution between $\dot{V}_{U\text{NO}}$, $D_{U\text{NO}}$, and conducting airway gas volume. Because the simple one-compartment model of the conducting airways so accurately predicts P_E at different values of \dot{Q}_E , use of more realistic models of the conducting airways is not likely to result in a better measurable prediction of the experimental data.

Lung Model Where NO Production Is Uniformly Distributed Throughout the Walls of the Conducting Airways

Tsoukias and George (28) reported what may be a more realistic model of the dynamics of pulmonary NO exchange in the conducting and alveolar airways. They define NO production as taking place uniformly throughout the walls of the lungs' tissues. From the differential mass balance of NO in the tissue, they derive a second-order partial differential equation (Eq. 1 in Ref. 28) that allows determination of the changes in P_E by interventions such as varying breath-holding time before exhalation, accelerating or slowing flow rates during exhalation, and varying the inspired NO concentration. Their experimental data obtained by measuring expired NO concentrations in seven normal subjects at different constant \dot{Q}_E levels result in a fit close to their model, similar to that obtained using *models 1* and *2* described above. Therefore, expired NO concentrations collected at different \dot{Q}_E in normal subjects unfortunately do not provide a means to determine which of these various models most closely accounts for the observed profiles of expired NO concentration.

Potential Errors in $\dot{V}_{L\text{NO}}$ Calculated With Eq. 2 With the Assumption That $D_{L\text{NO}}$ Is Constant

If the decrease with lung volume observed for $D_{L\text{CO}}$ is the same as that observed for $D_{L\text{NO}}$, $\dot{V}_{L\text{NO}}$ might be falsely high when values for $D_{L\text{NO}}$ obtained at high lung volumes are used and falsely low when measurements of $D_{L\text{NO}}$ measured at low lung volumes are used. In the calculation of $\dot{V}_{L\text{NO}}$ with Eq. 2, we used a mean value of $D_{L\text{NO}}$ obtained from $D_{L\text{NO}}$ continuously calculated from the expired NO concentration recorded during expiration. The calculation started at a maximum volume equal to the subject's TLC less four times the subject's estimated anatomic dead space and ended when the subject reached a volume equal to the RV plus 15% of the forced vital capacity (19, 20). Newth and co-workers (19) reported that $D_{L\text{CO}}$ measured with this method was unchanged as lung volume decreased. Preliminary measurements in nine subjects (20) showed that $D_{L\text{NO}}$ decreased 9% over this volume interval, but this change did not reach statistical significance ($P = 0.3$). Therefore, the change in $D_{L\text{NO}}$ with different lung volumes with use of the continuously calculated values during exhalation appears modest and would not be expected

to result in large errors in \dot{V}_{LNO} . However, use of single-breath measurements of \dot{D}_{LNO} obtained at TLC could result in overestimation of \dot{V}_{LNO} .

Fraction of Total \dot{V}_{LNO} and \dot{V}_{UNO} Measured From Analyses of P_E

This method of measuring \dot{V}_{LNO} and \dot{V}_{UNO} assumes that NO produced in the tissues enters the air spaces and then diffuses into the surrounding tissues and perfusing blood. Some of the NO produced in the alveoli and the conducting airways will react with the tissues and blood and never enter the air spaces (16). This NO will not be measured by analyses of NO in the airways; therefore, \dot{V}_{LNO} and \dot{V}_{UNO} are likely underestimates of the true amount of NO produced by the alveoli and conducting airways. We are unaware of methods that can measure the fraction of NO that does not communicate with airways, and its size may be increased by diseases that impair diffusion of NO from the tissues into the air spaces.

Comparison to Estimates of \dot{V}_{LNO} and PA From Data of Others

Because determination of PA requires breath holding or rebreathing for 10–15 s to achieve a constant value as well as rapid exhalations, most published values of P_E do not permit calculations of PA. However, Silkoff and co-workers (24) measured P_E in 10 subjects at \dot{Q}_E of 1,550 ml/s preceded by a 30-s breath hold and obtained a P_E of $2.4 \pm 1.0 \times 10^{-6}$ Torr. With use of their mean data for P_E at slower \dot{Q}_E , extrapolation of their data to an infinite value for \dot{Q}_E gives PA of $1.9 \pm 0.8 \times 10^{-6}$ Torr, which is in close agreement with our value of $1.6 \pm 0.7 \times 10^{-6}$ Torr observed in our seven subjects.

Recently, Tsoukias and co-workers (28, 29) published a similar two-compartment model consisting of a nonexpansile compartment representing the conducting airways and an expansile compartment representing the alveolar region of the lungs. In their seven normal subjects, they determined PA from 8–12 measurements of P_E and \dot{Q}_E performed at constant values of \dot{Q}_E that varied from 175 to 600 ml/s. With an equation equivalent to Eq. 3, they calculated PA and the flux of NO from the tissues of the conducting airways to the lumen. For *model 1*, flux equals $\dot{V}_{UNO} - (P_E \cdot D_{UNO})$. By plotting $\dot{Q}_E [P_E \div (P_B - 47)]$ on the vertical axis vs. \dot{Q}_E on the horizontal axis, the intercept on the vertical axis equals flux and the slope equals $PA \div (P_B - 47)$. Their values of PA of $4.1 \pm 2.3 \times 10^{-6}$ Torr were significantly greater than $1.6 \pm 0.7 \times 10^{-6}$ Torr obtained in our seven normal subjects ($P = 0.025$). We have no explanation for the higher values of PA obtained by Tsoukias and co-workers. However, their flow rates ranged from only 175 to 600 ml/s, whereas \dot{Q}_E for the subjects of Silkoff et al. (24) and our subjects varied from 4 ml/s to as high as 1,550 ml/s. This greater range in \dot{Q}_E may provide more precision in determining PA.

Comparison to Estimates of \dot{V}_{UNO} and D_{UNO} From Data of Others

Only a few investigators have measured P_E at a number of different constant \dot{Q}_E that permit calculation

of \dot{V}_{UNO} or D_{UNO} . Silkoff and co-workers (24) reported P_E at nine different values of \dot{Q}_E between 4.2 and 1,550 ml/s in 10 subjects. Their data shown in Fig. 13 permit calculation of \dot{V}_{UNO} and D_{UNO} by use of Eq. 4 or 7. Note the similarity of their data to the findings in our subjects shown in Fig. 9. *Model 1* closely fit the data of Silkoff and co-workers, with a mean r^2 of 0.996 for their 10 subjects. \dot{V}_{UNO} from their data was 0.061 ± 0.056 $\mu\text{l}/\text{min}$ compared with 0.076 ± 0.053 $\mu\text{l}/\text{min}$ in our subjects and did not differ significantly ($P = 0.22$). D_{UNO} in their subjects was 0.4 ± 0.3 $\text{ml} \cdot \text{min}^{-1} \cdot \text{Torr}^{-1}$ compared with 0.4 ± 0.4 $\text{ml} \cdot \text{min}^{-1} \cdot \text{Torr}^{-1}$ in our subjects ($P = 0.61$). *Model 2* gave similar results with a close fit to the data ($r^2 = 0.995$). \dot{V}_{UNO} was 0.053 ± 0.039 $\mu\text{l}/\text{min}$ compared with 0.074 ± 0.052 $\mu\text{l}/\text{min}$ in our subjects ($P = 0.20$), and D_{UNO} was 0.5 ± 0.3 $\text{ml} \cdot \text{min}^{-1} \cdot \text{Torr}^{-1}$ vs. 0.5 ± 0.4 $\text{ml} \cdot \text{min}^{-1} \cdot \text{Torr}^{-1}$ in our subjects ($P = 0.46$). The data of Silkoff and co-workers and our data show a wide scatter for the values of \dot{V}_{UNO} and D_{UNO} in normal subjects, with coefficients of variation (CV) ranging from 60 to 90%. PA and \dot{V}_{LNO} show less scatter, with a CV on the order of 40%.

Tsoukias and co-workers (28, 29) calculated flux from the data in their seven subjects, as described above. With use of representative values of P_E in our subjects at \dot{Q}_E of 175–600 ml/s used by Tsoukias and co-workers, their values of flux would only be ~1–3% smaller than \dot{V}_{UNO} . Flux in their subjects was 0.043 ± 0.015 $\mu\text{l}/\text{min}$ and did not significantly differ from the values of \dot{V}_{UNO} of 0.070 ± 0.048 $\mu\text{l}/\text{min}$ in our subjects with use of the faster \dot{Q}_E shown in Fig. 8 ($P = 0.20$) or 0.077 ± 0.053 $\mu\text{l}/\text{min}$ with *model 1* ($P = 0.16$) or 0.074 ± 0.52 $\mu\text{l}/\text{min}$ with *model 2* ($P = 0.18$) with use of faster and slower \dot{Q}_E .

Evaluation of a Simplified Method to Measure \dot{V}_{UNO} by Use of Only Faster \dot{Q}_E

Measurement of \dot{V}_{UNO} with $\dot{Q}_E > 80$ –100 ml/s would have the advantage of fewer measurements of P_E and elimination of the slow exhalations that are more difficult to perform because expiration must be continued for 25–150 s. The disadvantage is that D_{UNO} cannot

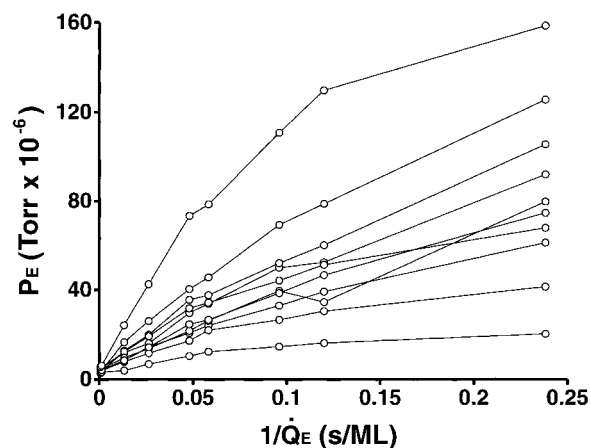


Fig. 13. P_E vs. $1/\dot{Q}_E$ in 10 subjects reported by Silkoff and co-workers (24). $\dot{Q}_E = 4.2$ –1,550 ml/s. Note similarity to data in Fig. 9 for our 7 subjects. Values for \dot{V}_{UNO} and D_{UNO} determined from these data are given in text.

be measured with any precision, because its accuracy requires the higher concentrations of NO in the conducting airways achieved with low values for \dot{Q}_E . In our subjects, $\dot{V}_{U_{NO}}$ calculated with only the faster \dot{Q}_E shown in Fig. 8 with use of Eq. 4 was 0.070 ± 0.048 $\mu\text{l}/\text{min}$ compared with 0.077 ± 0.053 $\mu\text{l}/\text{min}$ for *model 1* and 0.074 ± 0.052 $\mu\text{l}/\text{min}$ for *model 2* by use of all the values of P_E and \dot{Q}_E shown in Fig. 9. The three values did not differ significantly ($P = 0.2$) and have similar CVs of $\sim 70\%$. Measuring $\dot{V}_{U_{NO}}$ with the useful expediency of using only faster \dot{Q}_E provides acceptable values for $\dot{V}_{U_{NO}}$ but at the expense of measurements of $\dot{D}_{U_{NO}}$.

Choice of Analytic Method to Determine P_A , $\dot{V}_{U_{NO}}$, and $\dot{D}_{U_{NO}}$ From Measurements of P_E and \dot{Q}_E Performed at Different Constant \dot{Q}_E

Tsoukias and co-workers (28, 29) measured P_A and flux by plotting the quantity of NO exhaled, which is the product of \dot{Q}_E and $P_E \div (P_B - 47)$ vs. \dot{Q}_E , so that the slope of the graph equaled $P_A \div (P_B - 47)$ and the intercept equaled flux (Eq. 3). We rearranged Eq. 3 to the form in Eqs. 4 and 5 and plotted P_E vs. $1/\dot{Q}_E$ so that \dot{Q}_E did not appear on both axes, thus eliminating potential errors of mathematical coupling that can lead to erroneous conclusions (1, 22). However, in our normal subjects the two analytic techniques provide essentially the same values for $\dot{V}_{U_{NO}}$ or flux and P_A . For example, the data using the higher values of \dot{Q}_E shown in Fig. 8 with the analytic technique applied by Tsoukias and co-workers (28, 29) using Eq. 3 resulted in flux of 0.065 ± 0.045 $\mu\text{l}/\text{min}$ compared with $\dot{V}_{U_{NO}}$ of 0.070 ± 0.048 $\mu\text{l}/\text{min}$ by use of Eq. 5 ($P = 0.21$). P_A was $1.78 \pm 0.77 \times 10^{-6}$ Torr with the method of Tsoukias and co-workers compared with $1.60 \pm 0.72 \times 10^{-6}$ Torr with Eq. 6 ($P = 0.14$). Calculations with all seven sets of values of \dot{Q}_E and P_E resulted in flux of 0.067 ± 0.046 $\mu\text{l}/\text{min}$ with the method of Tsoukias and co-workers with use of Eq. 3 compared with $\dot{V}_{U_{NO}}$ of 0.077 ± 0.053 $\mu\text{l}/\text{min}$ with Eq. 4. Therefore, in normal subjects the two analytic methods result in similar data. Measurements in less well-trained subjects are prone to greater variations in P_E and \dot{Q}_E ; therefore, it may be wise to analyze data with both methods to determine whether mathematical coupling is influencing the results.

Alternate Models to Explain Expired NO Levels at Different \dot{Q}_E

The models shown in Figs. 2 and 5 precisely predict expired NO concentrations in normal subjects. An alternate model of NO exchange in the upper conducting airways has been proposed that in preliminary reports shows a similar close fit to the experimental data (15, 25). These authors assume that the NO production in the conducting airways results from a constant partial pressure of NO in the tissue wall (P_{ti}) that can diffuse into the lumen at a rate proportional to the concentration gradient. Then, for any small segment of the conducting airways of volume fV

$$\frac{d}{dt} fV \cdot \frac{P_U}{P_B - 47} = f\dot{D}_{U_{NO}} (P_{ti} - P_U) \quad (8)$$

where P_U is the partial pressure of NO in the segment and $f\dot{D}_{U_{NO}}$ is the diffusing capacity for NO of the segment. The solution of Eq. 8 is essentially the same as described in APPENDIX B and results in

$$P_E = (P_{ti} - P_A) \left[1 - e^{-\frac{\dot{D}_{U_{NO}} (P_B - 47)}{\dot{Q}_E}} \right] + P_A \quad (9)$$

The only difference from Eq. 7 describing the model in Fig. 5 is that the term P_{ti} replaces $\dot{V}_{U_{NO}} \div \dot{D}_{U_{NO}}$. Because all the other terms in Eqs. 7 and 9 are identical, P_{ti} in this model must equal $\dot{V}_{U_{NO}} \div \dot{D}_{U_{NO}}$ in *model 2* described above. Because the two models result in identical solutions, the only difference in the models is the terminology assigned to the measured constants. For example, if the model with constant NO concentration in the wall of the conducting airways (P_{ti}) is preferred, the value for P_{ti} is readily determined by dividing $\dot{V}_{U_{NO}}$ by $\dot{D}_{U_{NO}}$ obtained with *model 1* or *model 2*. In our subjects this value was 562 ± 798 and $313 \pm 437 \times 10^{-6}$ Torr for *models 1* and *2*, respectively. In the 10 subjects of Silkoff et al. (24) shown in Fig. 13, this value was 573 ± 798 and $289 \pm 531 \times 10^{-6}$ Torr for *models 1* and *2*, respectively.

In conclusion, these experiments show that NO production into the lungs' airways can be measured and divided into contributions from the alveoli ($\dot{V}_{L_{NO}}$) and the conducting airways ($\dot{V}_{U_{NO}}$). $\dot{V}_{L_{NO}}$ shows less scatter in measurements in normal subjects and is two- to fourfold greater than $\dot{V}_{U_{NO}}$. $\dot{D}_{L_{NO}}$ is >100 -fold greater than $\dot{D}_{U_{NO}}$. Because diffusion and control of NO production in the alveoli and conducting airways are likely governed by different mechanisms, this technique may provide new information about processes that control and alter NO production by the lungs.

APPENDIX A

Rate of Mixing of Alveolar Airway NO With Conducting Airway NO in a Two-compartment Model

Model 1 assumes that, at the initiation of expiration at a constant flow rate, NO in the conducting airways rapidly arrives at a constant value that is maintained throughout expiration. To determine the time required to reach this constant value, we calculated the rate of change of NO in the conducting airways (P_E) as NO enters from the alveolar airways. This instantaneous rate of change in the amount of NO in the conducting airways equals $d/dt[(P_E \cdot K)/(P_B - 47)]$, where K is the volume of gas in the conducting airways and P_E is the partial pressure of NO in the conducting airways. In this model, P_E is determined by four variables: 1) NO from the alveoli entering the conducting airways at a constant flow rate [$\dot{Q}_E \cdot P_A \div (P_B - 47)$], 2) NO produced in the conducting airway that enters its lumen ($\dot{V}_{U_{NO}}$), 3) NO diffusing out of the lumen of the conducting airway into the surrounding tissues ($P_E \cdot \dot{D}_{U_{NO}}$), and 4) NO leaving the conducting airway via exhalation [$\dot{Q}_E \cdot P_E \div (P_B - 47)$]. Therefore

$$\left(\frac{d}{dt} \right) \left(\frac{P_E \cdot K}{P_B - 47} \right) = \left(\frac{\dot{Q}_E \cdot P_A}{P_B - 47} \right) + \dot{V}_{U_{NO}} - P_E \cdot \dot{D}_{U_{NO}} - \left(\frac{\dot{Q}_E \cdot P_E}{P_B - 47} \right) \quad (A1)$$

This can be rearranged

$$\frac{dPE}{dt} = \frac{1}{K} (\dot{Q}_E \cdot PA + \dot{V}_{U_{NO}} [PB - 47]) - PE \cdot \frac{1}{K} [\dot{Q}_E + DU_{NO} (PB - 47)] \quad (A2)$$

Equation A2 has the form $dx/dt = a - bx$, the solution of which is $x = (a/b)(1 - e^{-bt})$ or

$$PE = \frac{\dot{Q}_E \cdot PA + \dot{V}_{U_{NO}} (PB - 47)}{\dot{Q}_E + DU_{NO} (PB - 47)} \left\{ 1 - e^{-\frac{[\dot{Q}_E \cdot DU_{NO} (PB - 47)]t}{K}} \right\} \quad (A3)$$

When t is large, the exponent approaches zero and Eq. A3 becomes identical to Eq. 4. Because the expression $[\dot{Q}_E \cdot PA + \dot{V}_{U_{NO}} (PB - 47)] / [\dot{Q}_E + DU_{NO} (PB - 47)]$ in Eq. A3 equals the value of PE when mixing is complete ($PE = \infty$), Eq. A3 can be written as

$$\frac{PE_t}{PE_\infty} = 1 - e^{-\frac{[\dot{Q}_E \cdot DU_{NO} (PB - 47)]t}{K}} \quad (A4)$$

where PE_t is PE at a selected time after initiation of exhalation. To estimate K in Eq. A4, we use the mean values obtained in our seven subjects for DU_{NO} of $0.5 \text{ ml} \cdot \text{min}^{-1} \cdot \text{Torr}^{-1}$ and the measured half time to reach a steady state during exhalation at $\dot{Q}_E = 250 \text{ ml/min}$ that equaled 0.25 min measured in one of the subjects. Then, according to Eq. A4

$$1 \div 2 = 1 - e^{-\frac{[250 + 0.5 (PB - 47)]0.25}{K}} \text{ or } K = 220 \text{ ml}$$

Then for any assumed flow rate \dot{Q}_E , the time to reach a specified ratio of PE to PE_∞ can be calculated. For example, if \dot{Q}_E is 1,000 ml/s (60,000 ml/min), $PB = 760 \text{ Torr}$, and the time to reach 99% equilibrium is desired, Eq. A4 becomes

$$\frac{99}{100} = 1 - e^{-\frac{[60,000 + 0.5(713)]t}{220}} \text{ or } t = 1.01 \text{ s}$$

In these experiments, expired volume in our subjects was $\sim 3,500 \text{ ml STPD}$. At this \dot{Q}_E of 1,000 ml/s, total time to exhale the breath is $3,500 \div 1,000$ or 3.5 s. Therefore, in this subject, 99% equilibrium in PE is reached when $1.01 \div 3.5$ or 29% of the breath has been exhaled. Figure 14 shows the required percentage of the breath exhaled to reach 99% and 99.9% equilibrium at different \dot{Q}_E with use of the above representative values for DU_{NO} of $0.5 \text{ ml} \cdot \text{min}^{-1} \cdot \text{Torr}^{-1}$ and K of 220 ml in our subjects. At $\dot{Q}_E \geq 80 \text{ ml/s}$, 29% of the breath must be exhaled to achieve 99% mixing and 43% must be exhaled for 99.9% mixing. At slower flow rates, mixing is achieved at progressively smaller fractions of the exhaled breath, because PA is a smaller fraction of the higher levels of NO present in the conducting airways with slow exhalations. In summary, this analysis shows that stable values for PE can be expected once 30–40% of the expiratory vital capacity is exhaled.

APPENDIX B

Determination of PE in a Two-compartment Model of the Airways with Stratification of the Concentration of NO Along the Lumen of the Conducting Airways

In any segment of the conducting airways illustrated in Fig. 5

$$\frac{d}{dt} fK \frac{PU_1}{PB - 47} = f\dot{V}_{U_{NO}} - fDU_{NO} \cdot PU_1 \quad (B1)$$

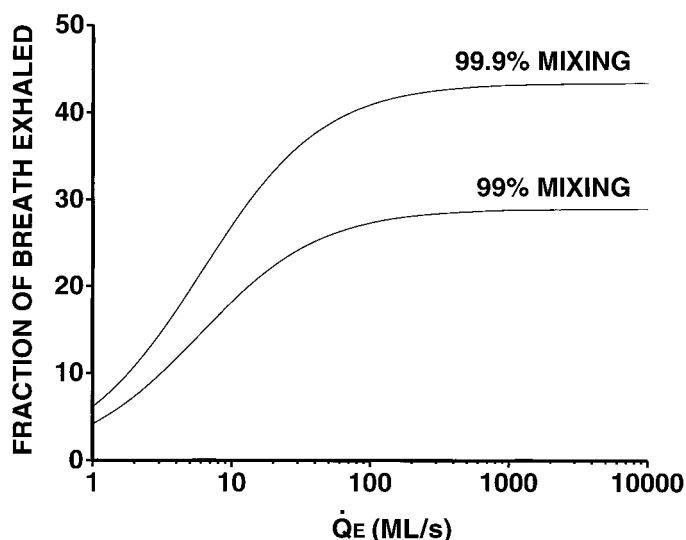


Fig. 14. Percentage of exhaled vital capacity required to reach a constant concentration of NO that is maintained during remainder of exhalation. At exhalations $>80 \text{ ml/s}$, 99% mixing is achieved when 29% of breath has been expired and 99.9% mixing when 43% has been expired. At slower \dot{Q}_E , mixing is achieved more quickly, because PA is a smaller fraction of higher levels of NO in conducting airways.

where fK is a small fraction of the total volume of gas in the conducting airway (K), $f\dot{V}_{U_{NO}}$ is the same small fraction of $\dot{V}_{U_{NO}}$, fDU_{NO} is the same small fraction of DU_{NO} , and PU_1 is the partial pressure of NO in the segment. The ratio of fK , $f\dot{V}_{U_{NO}}$, and fDU_{NO} is assumed constant throughout the conducting airways. As this volume of gas moves to the next segment, $f\dot{V}_{U_{NO}}$ will add NO and NO will be removed at a rate equal to $fDU_{NO} \cdot PU_2$, where PU_2 is the partial pressure of NO in the next segment that resulted from residence in the previous segment. In Eq. B1, the term f cancels out, because each segment is defined as containing an equal fraction f of K , $\dot{V}_{U_{NO}}$, and DU_{NO} . Rearranging gives

$$\frac{d}{dt} PU = \frac{\dot{V}_{U_{NO}} (PB - 47)}{K} - \frac{PU \cdot DU_{NO} (PB - 47)}{K} \quad (B2)$$

Equation B2 is of the form $dx/dt = a - bx$. If the initial value of PU is assumed to be zero, this type of equation has the solution

$$x = (a \div b) (1 - e^{-bt})$$

or

$$PU = \frac{\dot{V}_{U_{NO}}}{DU_{NO}} \left[1 - e^{-\frac{DU_{NO} (PB - 47)t}{K}} \right] \quad (B3)$$

where PU is the partial pressure of NO at the end of the conducting airways and equals PE, the expired partial pressure of NO. The term t is the time for the segment to traverse the conducting airways and equals the transit time for NO through the conducting airways. The volume of the conducting airways (K) divided by t equals \dot{Q}_E or

$$PE = \frac{\dot{V}_{U_{NO}}}{DU_{NO}} \left[1 - e^{-\frac{DU_{NO} (PB - 47)}{\dot{Q}_E}} \right] \quad (B4)$$

Equation B4 states that as \dot{Q}_E approaches zero, PE reaches a maximum value of $\dot{V}_{U_{NO}} \div DU_{NO}$. This value results because when there is no flow in the upper airways, the amount of NO

entering ($\dot{V}_{U_{NO}}$) will equal the amount leaving, which equals $PE \cdot \dot{D}_{U_{NO}}$ or $\dot{V}_{U_{NO}} = PE \cdot \dot{D}_{U_{NO}}$. Rearranging, $PE = \dot{V}_{U_{NO}} \div \dot{D}_{U_{NO}}$ when $\dot{Q}_E = 0$. When \dot{Q}_E is very fast, Eq. B4 states that PE approaches zero. However, unlike Eq. B3, a finite concentration of NO equal to P_A is entering the conducting airways from the alveoli, so when \dot{Q}_E is infinitely fast, PE equals P_A , not zero. Therefore, the correct limits for PE are as follows: P_A when \dot{Q}_E approaches infinity and $\dot{V}_{U_{NO}} \div \dot{D}_{U_{NO}}$ when \dot{Q}_E approaches zero. Equation B4 can therefore be expanded to

$$PE = \left(\frac{\dot{V}_{U_{NO}}}{\dot{D}_{U_{NO}}} - P_A \right) \left[1 - e^{-\frac{\dot{D}_{U_{NO}} (P_B - 47)}{\dot{Q}_E}} \right] + P_A \quad (B5)$$

The authors thank Dr. Phillip E. Silkoff for providing the values of expired NO at different expiratory flow rates previously reported in Ref. 24 and illustrated in Fig. 13. Ann Bauman contributed expert editorial assistance.

This study was supported by National Institutes of Health Grants R01-HL-51701, R01-ES-02679, and T32-HL-07216.

Address for reprint requests and other correspondence: A. P. Pietropaoli, Pulmonary and Critical Care Unit, University of Rochester Medical Center, 601 Elmwood Ave., Box 692, Rochester, NY 14642-8692 (E-mail: anthony_pietropaoli@urmc.rochester.edu).

Received 12 January 1999; accepted in final form 14 June 1999.

REFERENCES

1. Archie, P. A., Jr. Mathematical coupling of data: a common source of error. *Ann. Surg.* 193: 296–303, 1981.
2. Crapo, R. O., A. H. Morris, and R. M. Gardner. Reference spirometric values using techniques and equipment that meet ATS recommendations. *Am. Rev. Respir. Dis.* 123: 659–664, 1981.
3. Cremona, G., T. Higenbottam, C. Borland, and B. Mist. Mixed expired nitric oxide in primary pulmonary hypertension in relation to lung diffusion capacity. *Q. J. Med.* 87: 547–551, 1994.
4. Cremona, G., T. Higenbottam, M. Takao, L. Hall, and E. A. Bower. Exhaled nitric oxide in isolated pig lungs. *J. Appl. Physiol.* 78: 59–63, 1995.
5. DuBois, A. B., S. Y. Botelho, G. N. Bedell, R. M. Marshall, and J. H. Comroe. A rapid plethysmographic method for measuring thoracic gas volume: a comparison with a nitrogen washout method for measuring functional residual capacity in normal subjects. *J. Clin. Invest.* 35: 322–326, 1956.
6. DuBois, A. B., P. M. Kelley, J. S. Douglas, and V. Mohsenin. Nitric oxide production and absorption in trachea, bronchi, bronchioles, and respiratory bronchioles of humans. *J. Appl. Physiol.* 86: 159–167, 1999.
7. Fallon, M. B., G. A. Abrams, B. Luo, Z. Hou, J. Dai, and D. D. Ku. The role of endothelial nitric oxide synthase in the pathogenesis of a rat model of hepatopulmonary syndrome. *Gastroenterology* 113: 606–614, 1997.
8. Fletcher, R. *Practical Methods of Optimization* (2nd ed.). New York: Wiley, 1987, p. 49–57.
9. Geigel, E. J., R. W. Hyde, I. B. Perillo, A. Torres, P. T. Perkins, A. P. Pietropaoli, L. M. Frasier, M. W. Frampton, and M. J. Utell. Rate of nitric oxide production by the lower airway of human lungs. *J. Appl. Physiol.* 86: 211–221, 1999.
10. Giad, A., and D. Saleh. Reduced expression of endothelial nitric oxide synthase in the lungs of patients with pulmonary hypertension. *N. Engl. J. Med.* 333: 214–221, 1995.
11. Guo, F. H., H. R. DeRaeve, T. W. Rice, D. J. Stuehr, F. B. J. M. Thunnissen, and S. C. Erzurum. Continuous nitric oxide synthesis by inducible nitric oxide synthase in normal human airway epithelium in vivo. *Proc. Natl. Acad. Sci. USA* 92: 7809–7813, 1995.
12. Hyde, R. W., E. J. Geigel, A. J. Olszowka, J. A. Krasney, R. E. Forster II, M. J. Utell, and M. W. Frampton. Determination of production of nitric oxide by lower airways of humans—theory. *J. Appl. Physiol.* 82: 1290–1296, 1997.
13. Kharitonov, S., K. Alving, and P. J. Barnes. Exhaled and nasal nitric oxide measurements: recommendations. *Eur. Respir. J.* 10: 1683–1693, 1997.
14. Kimberly, B., B. Negadnik, G. D. Giraud, and W. E. Holden. Nasal contribution to exhaled nitric oxide at rest and during breathholding in humans. *Am. J. Respir. Crit. Care Med.* 153: 829–836, 1996.
15. Kirsten, A. M., R. A. Jörres, D. Kirsten, and H. Magnussen. Determination of bronchial nitric oxide (NO) concentrations in subjects with mild asthma and healthy subjects (Abstract). *Am. J. Respir. Crit. Care Med.* 155: A825, 1997.
16. Lancaster, J. R., Jr. A tutorial on the diffusibility and reactivity of free nitric oxide. In: *Nitric Oxide: Biology and Chemistry*. San Diego, CA: Academic, 1997, vol. 1, p. 18–30.
17. Massaro, A. F., B. Gaston, D. Kita, C. Fanta, J. S. Stamler, and J. M. Drazen. Expired nitric oxide levels during treatment of acute asthma. *Am. J. Respir. Crit. Care Med.* 152: 800–803, 1995.
18. Matsumoto, A., K. Ogura, H. Yasunobu, M. Kakoki, F. Watanabe, K. Takenaka, Y. Shiratori, S. Momomura, and M. Omata. Increased nitric oxide in the exhaled air of patients with decompensated liver cirrhosis. *Ann. Intern. Med.* 123: 110–113, 1995.
19. Newth, C. J. L., D. J. Cotton, and J. A. Nadel. Pulmonary diffusing capacity measured at multiple intervals during a single exhalation in man. *J. Appl. Physiol.* 43: 617–625, 1977.
20. Perillo, I. B., J. S. Olszowka, A. P. Pietropaoli, A. Torres, P. T. Perkins, M. J. Utell, M. W. Frampton, and R. W. Hyde. Comparison of nitric oxide diffusing capacity calculated by rebreathing and single breath exhalation for the measurements of nitric oxide production by the lungs (Abstract). *Am. J. Respir. Crit. Care Med.* 157: A713, 1998.
21. Riley, M. S., J. Pórszász, J. Miranda, M. P. K. J. Engelen, B. Brundage, and K. Wasserman. Exhaled nitric oxide during exercise in primary pulmonary hypertension and pulmonary fibrosis. *Chest* 111: 44–50, 1997.
22. Ronco, J. J., P. T. Phang, K. R. Walley, B. Wiggs, J. C. Fenwick, and J. A. Russell. Oxygen consumption is independent of changes in oxygen delivery in severe adult respiratory distress syndrome. *Am. Rev. Respir. Dis.* 143: 1267–1273, 1991.
23. Silkoff, P. E., P. A. McClean, M. Caramori, A. S. Slutsky, and N. Zamel. A significant proportion of exhaled nitric oxide arises in large airways in normal subjects. *Respir. Physiol.* 113: 33–38, 1998.
24. Silkoff, P. E., P. A. McClean, A. S. Slutsky, H. G. Furlott, E. Hoffstein, S. Wakita, K. R. Chapman, J. P. Shalal, and N. Zamel. Marked flow-dependence of exhaled nitric oxide using a new technique to exclude nasal nitric oxide. *Am. J. Respir. Crit. Care Med.* 155: 260–267, 1997.
25. Silkoff, P. E., J. T. Sylvester, N. Zamel, and S. Permutt. Nitric oxide diffusion in the human airway (Abstract). *Ann. Biomed. Eng.* 26, Suppl. 1: S47, 1998.
26. Stewart, T. E., F. Valenza, S. P. Ribeiro, A. D. Wener, G. Volgyesi, J. B. M. Mullen, and A. S. Slutsky. Increased nitric oxide in exhaled gas as an early marker of lung inflammation in a model of sepsis. *Am. J. Respir. Crit. Care Med.* 151: 713–718, 1995.
27. Stitt, J. T., A. B. Dubois, J. S. Douglas, and S. G. Shimada. Exhalation of gaseous nitric oxide by rats in response to endotoxin and its absorption by the lungs. *J. Appl. Physiol.* 82: 305–316, 1997.
28. Tsoukias, N. M., and S. C. George. A two-compartment model of pulmonary nitric oxide exchange dynamics. *J. Appl. Physiol.* 85: 653–666, 1998.
29. Tsoukias, N. M., Z. Tannous, A. F. Wilson, and S. C. George. Single-exhalation profiles of NO and CO₂ in humans: effect of dynamically changing flow rate. *J. Appl. Physiol.* 85: 642–652, 1998.
30. Watkins, D. N., D. J. Peroni, K. A. Basclain, M. J. Garlepp, and P. J. Thompson. Expression and activity of nitric oxide synthases in human airway epithelium. *Am. J. Respir. Cell Mol. Biol.* 16: 629–639, 1997.
31. Weibel, E. R. *Morphometry of the Human Lung*. New York: Academic, 1963, p. 136–148.